Nonlinear System Modeling and Velocity Feedback Compensation for Effective Force Testing

Jian Zhao, S.M.ASCE[1]; Carol Shield, M.ASCE[2]; Catharine French, M.ASCE[3]; and Thomas Posbergh[4]

Abstract: Effective force testing (EFT) is a test procedure that can be used to apply real-time earthquake loads to large-scale structural models. The implementation of the EFT method requires velocity feedback compensation for the actuators in order to apply forces accurately to test structures. Nonlinearities in the servosystem have a significant impact on the velocity feedback compensation and test results when large flow demands are present, which can be caused by large structural velocities and/or large forces applied to the test structure. This paper presents a nonlinear servosystem model, upon which a nonlinear compensation scheme is proposed. The model and compensation scheme are experimentally verified. The results indicate that the proposed model accurately describes the servosystem behavior, and with the nonlinear velocity feedback compensation, real-time dynamic testing can be conducted using the EFT method.

DOI: XXXX

CE Database subject headings: Dynamic tests; Simulation models; Earthquakes; Structural response; Velocity; Damping.

Introduction

Computer simulation has been widely used in evaluating control algorithms for seismic mitigation with passive or semiactive damping devices; however, the accuracy of the results depends on the characterization of the energy dissipation components. Hence real-time dynamic testing is necessary for assessing the behavior of structures employing velocity dependent devices under seismic loadings. A shake table is often used to simulate the dynamic effects of earthquakes on structural models. However, structures tested on shake tables typically have to be scaled down due to limited table capacities. At smaller scales, structural details such as connections cannot be represented realistically, and energy dissipation of structural control devices may not be demonstrated accurately.

Effective force testing (EFT) is a dynamic test procedure to apply real-time earthquake loads to large-scale structures that can be simplified as lumped mass systems. In an EFT test, the test structure is anchored to a stationary base, and dynamic forces are applied by hydraulic actuators to the center of each story mass of the structure. The force to be imposed (effective force) is the product of the structural mass and the ground acceleration record, and thus is independent of the structural properties such as stiffness and damping, and their changes during the test. Motions measured relative to the ground are equivalent to the response that a structure can develop relative to a moving base as in a shake table test or an earthquake event.

The development and implementation of EFT has been underway at the University of Minnesota since 1996. Early direct application of the EFT method on a linear elastic structural model indicated that the actuator was not able to apply forces accurately near the natural frequency of the test structure (Dimig et al. 1999). The concept of *natural velocity feedback* (i.e., the interaction between the actuator piston velocity and the actuator control) identified by Dyke et al. (1995) was used to explain the problem: the actuator is controlled by a servovalve through hydraulic flow under pressure, and the differential pressure inside the actuator chambers causes the force applied to the test structure. The actuator chamber volumes change due to the actuator piston in motion with the structure, resulting in unwanted chamber pressure variation. Standard proportional-integral-derivative (PID) controllers are unable to compensate for the pressure variation, thus causing force-tracking errors.

Velocity feedback compensation can solve this problem and make the successful implementation of EFT possible (Shield et al. 2001). In the solution, the effect of the natural velocity feedback is compensated by modifying the command to the servovalve. The chamber volume change to be compensated is determined as the product of the measured piston/structure velocity and the piston area. The compensation signal is convolved with the inverse of the forward system dynamics, and then added to the force command. The modified command signal compensates for the effect of the piston motion after going through the forward dynamics. The compensation is independent of the structural properties (i.e., damping and stiffness) and their changes during a test.

Previous implementation of the EFT method (e.g., Timm 1999) was limited to tests with small hydraulic demands, for which the servovalve operated in the linear range of its behavior. For tests with large flow demands, nonlinearities of the servosystem can have significant impact on the performance of the velocity feedback compensation (Zhao et al. 2003a, b). The servosystem nonlinearities become significant when a test involves large

[1]Research Associate, Dept. of Civil Engineering, Iowa State Univ., Ames, IA 50011. E-mail: zhao0058@iastate.edu

[2]Professor, Dept. of Civil Engineering, Univ. of Minnesota, Minneapolis, MN. E-mail: cfrench@umn.edu

[3]Associate Professor, Dept. of Civil Engineering, Univ. of Minnesota, Minneapolis, MN. E-mail: ckshield@umn.edu

[4]Associate Professor, Dept. of Electrical and Computer Engineering, Univ. of Minnesota, Minneapolis, MN. E-mail: posbergh@umn.edu

Note. Associate Editor: Eric N. Landis. Discussion open until August 1, 2005. Separate discussions must be submitted for individual papers. To extend the closing date by one month, a written request must be filed with the ASCE Managing Editor. The manuscript for this paper was submitted for review and possible publication on October 13, 2003; approved on May 11, 2004. This paper is part of the ***Journal of Engineering Mechanics***, Vol. 131, No. 3, March 1, 2005. ©ASCE, ISSN 0733-9399/2005/3-1–XXXX/$25.00.

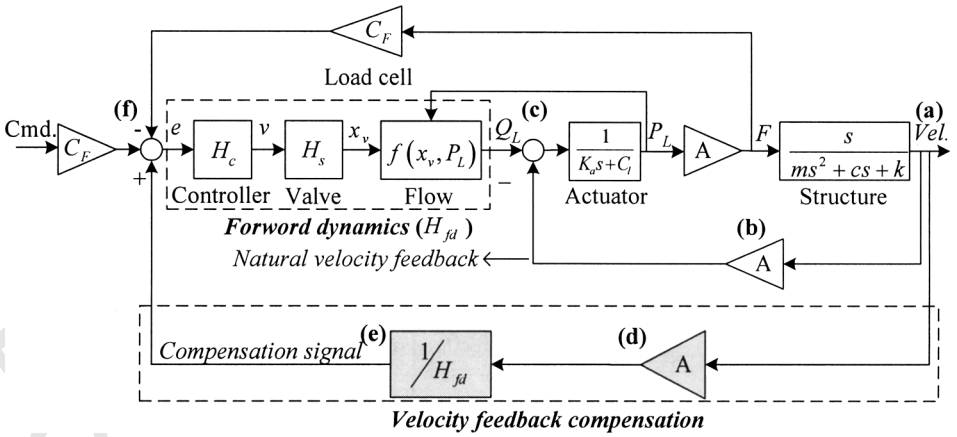

Fig. 1. Block diagram model of the test system

forces and/or large velocities compared to the actuator/servovalve capacities, which usually causes large hydraulic flow demands. Hence nonlinear velocity feedback compensation is necessary to extend the EFT method to fully utilize the test equipment. A detailed mathematical model of the test system is necessary for designing nonlinear compensation algorithms.

This paper first presents a nonlinear model for a servosystem (i.e., an actuator and its servovalve) including the identification of two important parameters, the response delay and flow property of the servovalve. The models are expressed in block diagrams and transfer functions, which represent the input/output relations described by ordinary differential equations in the frequency domain (Franklin et al. 1994). A nonlinear compensation scheme is then proposed and validated through experiments. Finally, the effects of the two critical parameters on the system performance are discussed along with related stability problems.

System Modeling

Test System Model

The dynamic models of a servohydraulic actuator attached to a single degree-of-freedom (SDOF) structure have been derived by Zhao et al. (2002) based on the formulations by Merritt (1967). Fig. 1 presents the block diagram model of the test system with velocity feedback compensation. This figure shows the relations between system components (blocks with inputs and outputs labeled), including the interaction between the actuator piston velocity and the actuator control. During a test, the servovalve controller compares a force command signal to a force feedback signal (both converted to voltage signals by C_F) and sends an amplified error signal (v) to the servovalve (H_s) to drive the valve spool (x_v). The spool regulates the hydraulic flow entering the actuator (Q_L), causing differential pressure across the actuator piston (P_L). The pressure difference multiplied by the piston area (A) produces the force (F) applied to the test structure. The force measured by a load cell on the actuator piston is finally fed back to the controller to close the control loop.

The natural velocity feedback is shown by the loop (a)-(b)-(c) from the structural velocity to the summing point (c), which represents the law of conservation of mass: the hydraulic flow into the actuator needs to counteract the fluid compressibility (K_a), system leakage (C_l), and chamber volume change ($A\dot{x}$). The effect of the natural velocity feedback loop (a)-(b)-(c) is compensated by a positive feedback loop (a)-(d)-(e)-(f). In order to cancel the effect of the natural velocity feedback at point (c), the compensation loop needs to incorporate the inverse of the dynamics between (f) and (c) (forward dynamics H_{fd}), which represents the behavior of the servovalve and its controller. Therefore the servovalve and its controller need to be characterized in detail.

Servovalve Controller

The major function of the servovalve controller is the amplification of the error signal (e) through PID control. The controller I-gain was set to zero in this study because time variant behavior of the structure was under investigation and the I-gain is typically used to reduce the steady-state tracking error of the system. The servovalve controller (H_c) for PID control with zero I-gain can be described by

$$H_c = \frac{v}{e} = G_p + G_d s \tag{1}$$

where s=complex variable (usually $j\omega$ where ω represents the frequency of system input and $j=\sqrt{-1}$) and G_p and G_d =proportional and derivative gains of the controller, respectively.

Servovalve Dynamics

A 5.7 L/s (90 gpm) three-stage MTS 256.09 servovalve was used in this study. The first stage (a torque motor armature) and the second stage (a spool-type valve) formed a two-stage servovalve that could be used as a functional unit. In the three-stage servovalve, the two-stage valve (also called the pilot-stage valve) controlled the spool position of the third stage (main-stage) valve through a displacement control loop. The relations between these valve components are shown by block diagrams in Fig. 2.

The pilot-stage valve was a 0.06 L/s (1 gpm) MTS 252.21 servovalve custom manufactured by Moog, Inc. Although it is possible to derive higher-order models for the pilot-stage valve including the dynamics of the individual valve components, such as in Nikiforuk et al. (1969), simple models have been used to capture the essential behavioral characteristics of Moog valves (Thayler 1965). In addition, it is only necessary for the model to represent the servovalve response up to approximately 20 Hz because the frequency range of interest is typically limited in large-

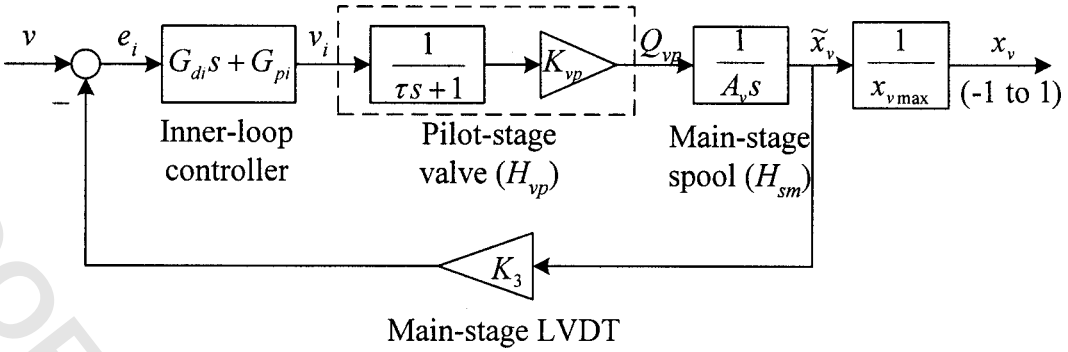

Fig. 2. Block diagram model of the three-stage servovalve (H_s)

scale structural testing (e.g., 0–10 Hz in this study). Therefore a first-order model was used to represent the dynamics of the pilot-stage valve

$$H_{vp} = \frac{Q_{vp}}{v_i} = \frac{K_{vp}}{\tau s + 1} \tag{2}$$

where τ=equivalent time constant of the pilot-stage valve. The pilot-stage valve flow property was lumped into the equation. It is appropriate to assume that the flow controlled by the pilot-stage valve (Q_{vp}) is proportional to the valve command (v_i) (Chen, personal communication, 2003); hence K_{vp} is the valve flow gain that relates the pilot-stage flow to the valve command.

The pilot-stage flow controlled the movement of the main-stage spool by causing differential pressure acting on the spool ends. It has been shown that the forces acting on the main-stage spool are typically small compared with the available driving force (the supply pressure), and the motion of the spool is small (a couple of millimeters) (Merritt 1967; Chen personal communication, 2003). Hence the effect of spool mass, friction, and other forces acting on the spool as well as the compressibility of the hydraulic fluid are deemed negligible (Thayler 1965). Consequently, the pilot-stage flow (Q_{vp}) was assumed equal to the main-stage spool velocity times the cross-sectional area of the main-stage spool

$$H_{sm} = \frac{\tilde{x}_v}{Q_{vp}} = \frac{1}{A_v s}, \tag{3}$$

where A_v=main-stage spool area and $\tilde{x}_v$=spool position of the main-stage valve.

The valve driver module inside the servovalve controller compares the desired spool position with the spool position feedback measured by an internal linear variable differential transformer (LVDT) with a sensitivity factor of K_3, and sends a current proportional to the difference between these two signals to the torque motor. A proportional-derivative (PD) controller is built into the valve control module to adjust the inner loop error signal (e_i). Following the tuning procedure of the servovalve recommended by the manufacturer, a unity proportional gain and a zero derivative gain were found suitable for the control of the servovalve; therefore the dynamics of the PD controller were neglected. Hence, by applying principles of operational algebra to the block diagram model shown in Fig. 2, the dynamics of the three-stage servovalve was derived as

$$H_s = \frac{x_v}{v} = \frac{K_{vp}}{\tau A_v s^2 + A_v s + K_3 K_{vp} x_{v\,\max}} \frac{1}{} \tag{4}$$

Note that the spool position of the main-stage valve ($\tilde{x}_v$) has a unit of length. It is often convenient to normalize the spool position by the maximum spool stroke $x_{v\,\max}$.

Servovalve Flow Property

The offset of the main-stage spool from its null position forms four orifices to allow hydraulic flow as shown in Fig. 3(a). The configurations of these load and leakage flows are shown in Figs. 3(b and c), respectively. In the case presented in Fig. 3(a), hydraulic fluid flows into the right chamber of the actuator and out of the left chamber through two load flow orifices. In the meantime, leakage flow through a different type of orifice exists from the right chamber to the return line and from the supply line to the left chamber. Using the orifice flow equations from Merritt (1967), the relationship between the main-stage spool opening and the flow to the actuator for spool openings to the right in Fig. 3 was formulated as

$$Q_1, Q_2 = C_d w x_v \sqrt{\frac{1}{\rho}(P_s - P_L)} - \frac{\pi r c^3}{6\mu x_v}\left[1 + \frac{3}{2}\left(\frac{e}{c}\right)^2\right]\frac{P_s + P_L}{2} \tag{5}$$

where C_d=discharge coefficient of the load flow orifice, w=area gradient (perimeter) of the valve spool, P_s=hydraulic pressure supply, P_L=load pressure (pressure difference across the actuator piston, $P_1 - P_2$), ρ=mass density of the hydraulic fluid, r, c, and e=geometric coefficients of the leakage orifice illustrated in Fig. 3(c), and μ=fluid viscosity. A detailed derivation of the equation can be found in Zhao (2003).

The second part of Eq. (5) represents the valve leakage flow (Q_{lv}), which can be viewed as a flow deduction from the flow controlled by the servovalve (Q_L) (e.g., $Q_1 = Q_L - Q_{lv}$ for the right chamber in Fig. 3). Hence the leakage flow was neglected in characterizing the flow property of the servovalve, and was considered in the analysis of the actuator dynamics as discussed later. After considering the direction of the spool opening, the servovalve flow was described by

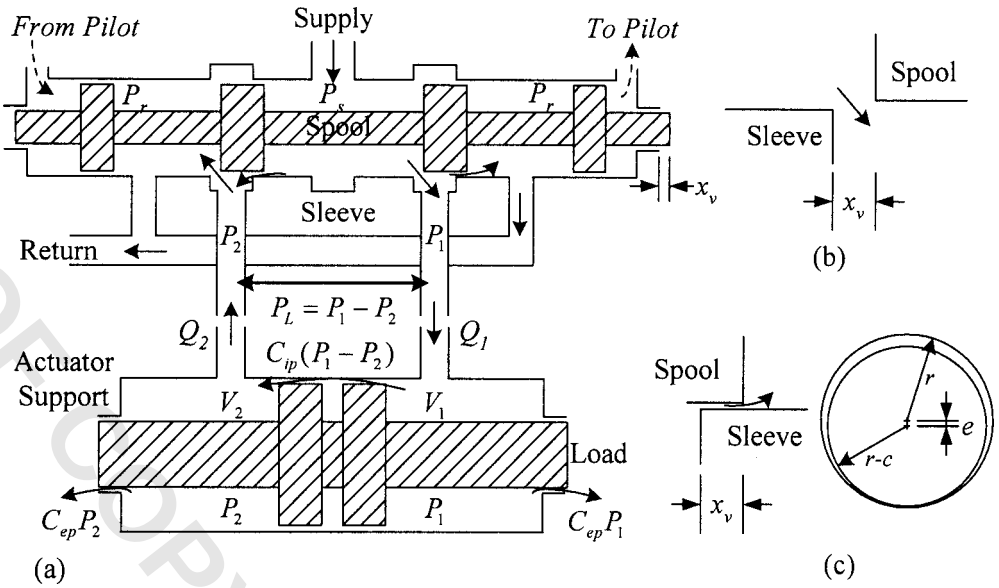

Fig. 3. (a) Schematic of the main-stage valve spool with actuator piston (structure attached to the right side); (b) load flow orifice; and (c) leakage flow orifice

$$Q_L = K_v x_v \sqrt{1 - \frac{x_v}{|x_v|}\frac{P_L}{P_s}} \tag{6}$$

where $K_v = (C_d w \sqrt{1/\rho})\sqrt{P_s}$ is called the flow gain of the servovalve.

The piston of a double acting actuator is schematically shown in Fig. 3(a). In this case, the servovalve spool opening was assumed positive (to the right in Fig. 3), which caused hydraulic fluid flow into the right chamber of the actuator, thus raising the pressure on the right side of the actuator piston and reducing the pressure on the left side. The resulting pressure difference caused a tension force in the actuator piston, which is defined herein as a positive force.

By applying the law of conservation of mass to the control volumes (V_1 and V_2) in both actuator chambers, the linearized actuator dynamics were found to be (Zhao 2003)

$$Q_L = K_a \dot{P}_L + C_l P_L + A\dot{x} \tag{7}$$

where K_a=compressibility coefficient of the hydraulic fluid inside the actuator chambers, and C_l represents the system leakage, which includes the servovalve leakage shown in the second part of Eq. (5), actuator cross-port (internal) leakage, and actuator external leakage (actuator chambers to the drain line). The actuator leakage can be described using a similar equation as that for the servovalve leakage because their passages are similar to the valve leakage orifice. The leakage descriptions in Eq. (5) indicated that part of the total leakage (represented by C_l) is related to the load pressure (proportional leakage), and the other part is related to the pressure supply (constant leakage). The proportional leakage [shown in Eq. (7) by coefficient C_l] was found to be equivalent to damping of the actuator dynamics; while the constant leakage could significantly deteriorate the force tracking ability of the actuator (Zhao 2003).

To facilitate the detailed analysis of the test system and the design of velocity feedback compensation schemes, parameters for the proposed models were identified, and are listed in Table 1. Among the parameters, the servovalve response delay and servovalve flow property were critical to the velocity feedback compensation.

Parameter Identification

Servovalve Response Delay

The response of the servovalve has an inevitable delay compared to its commands. For a second-order system shown in Eq. (4)

Table 1. Actuator, Servovalve, and Structure Properties

Parameter	Value
A	8.212E−3 m^2 (12.73 in.^{2})
A_v	1.964E−4 m^2 (0.3044 in.^{2})
c	4.33 kN/m/s (0.024 kips/in/s)
C_l	1.3E−8 m^3/s/ksi (5.5 in.^{3}/s/ksi)
C_F	0.056 V/kN (0.25 V/kip)
G_p	0.8059
G_d	0.002 s
k	693.8 kN/m (3.96 kips/in.)
K_3	3,579.13 V/m (90.91 V/in.)
K_a	7.56E−10 m^3/kPa (0.3182 in.^{3}/ksi)
K_s	0.1
K_v	1.64E−2 m^3/s (1,003 in.^{3}/s)
K_{vp}	1.06E−5 m^3/s/V (0.644 in.^{3}/s/V)
P_s	1.9E4 kPa (2.8 ksi)
T_d	5.0 ms
T_{ld}	5.6 ms
$x_{v\,\max}$	2.79E−3 m (0.11 in.)
α	0.1
τ	0.0014 s
ζ	0.964
ω_n	59 Hz

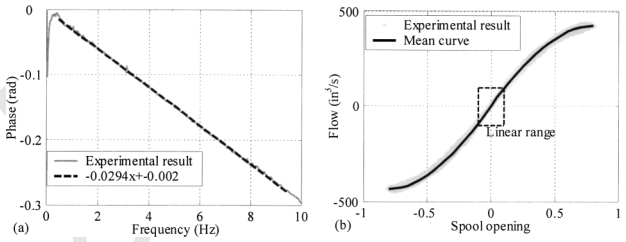

Fig. 4. (a) Servovalve response delay, and (b) nonlinear servovalve flow gain (1 in.^{3}/s=1.64E−5 m^3/s)

with the valve parameters (τ, A_v, K_3, K_{vp}, and $x_{v\,\max}$) listed in Table 1, the apparent natural frequency of the system (ω_n) was calculated as 59 Hz ($\sqrt{K_3K_{vp}/\tau A_v}/2\pi$), and the equivalent damping (ζ) was determined to be 96.4% of critical damping ($A_v/2\sqrt{K_3K_{vp}\tau A_v}$). Hence the response delay (T_d) was calculated to be 5.2 ms using $2\zeta/\omega_n$ for low frequencies.

To validate the identified response delay (T_d), a test was conducted, in which the actuator was in displacement control, and the actuator piston was kept in its neutral position by shutting off the hydraulic supply to the main-stage valve. The controller P gain was set to unity and the derivative gain set to zero, such that the valve command signal could be controlled without additional equipment. A sinesweep input (0–10 Hz in 32 s) with constant amplitude of 25 mm (1 in.) was chosen as the command signal. The valve command and inner loop feedback signal that represented the spool position were obtained from the servovalve controller. The phase difference of the two signals in the frequency domain shown in Fig. 4(a) indicated a linear relation between the phase lag (rad) and the input frequency (Hz) (note that below 0.25 Hz, the test could not capture the small phase differences due to measurement limitations). Hence the response delay was experimentally determined to be 4.7 ms by dividing the slope of the regression line by 2π.

The inconsistency in the above two estimations of the response delay was attributed to the fact that the pilot-stage flow gain (represented by K_{vp}) affected the servovalve dynamics. At small hydraulic demands such as in the above test, the flow gain was typically large, resulting in a faster response and smaller delay time. Fine tuning of the response delay (T_d) was done experimentally based on observations mentioned in the discussion section below. A response delay of 5 ms was used in the implementation. The servovalve flow property was another parameter that was affected by servosystem uncertainties.

Servovalve Flow Property

The servovalve flow was described by Eq. (6), which contains two major types of nonlinearity, *load pressure influence and nonlinear flow gain*. The load pressure influence is explicitly represented by the square root term in Eq. (6). It reflects the nonlinear relation between the flow through the servovalve load flow orifice and the pressure drop across the orifice. Bernoulli's theory was used to derive the orifice flow equation (Merritt 1967). The nonlinear flow gain describes the nonlinear flow discharge through a variable size orifice: the flow discharge rate decreases with an increase in orifice area (e.g., spool opening for the servovalve orifice). The nonlinear behavior is complicated such that an experimental identification is necessary.

Dynamically measuring the servovalve flow using a flow meter was deemed inappropriate because flow meters typically do not respond fast enough. Hence a flow curve (i.e., the flow controlled by servovalve Q_L versus the main-stage spool opening x_v) was constructed as follows. The actuator was set to displacement control with a unity controller P-gain and zero D-gain. Tests were conducted under no load condition (the structure was disconnected) such that the pressure difference across the actuator piston (load pressure P_L) was negligible. The spool opening was obtained directly by measuring the main-stage spool position while the corresponding flow was calculated using Eq. (7). Because the load pressure was negligible and its derivative was deemed (and proved during the tests) negligible, the flow calculation was further simplified as the piston velocity multiplied by the piston area ($A\dot{x}$). The piston velocity was calculated using the central difference method from the measured piston displacement. Because the constant leakage was typically negligible (less than 0.5% of valve capacity), the calculated flow in this procedure was equivalent to the flow controlled by the servovalve (Q_L).

To control the spool opening, sinusoidal inputs were used with a frequency of 3 Hz, at which the maximum valve command signal (also the system error) would be 90% of the command signal due to the overall system dynamics (Zhao 2003). Tests with 90% (4.5 in.), 80% (4 in.), 60% (3 in.), 40% (2 in.), and 20% (1 in.) full stroke command were conducted, and the result of the test with the 90% full stroke command is shown by the gray dots in Fig. 4(b). A piecewise linear curve was constructed by connecting 21 control points at an interval of 10% spool opening to represent the flow property of the servovalve. The flow values at the control points were calculated as the mean of the experimental results. The values of a typical flow curve are listed in Table 2 in which a linear extrapolation was used to generate the points beyond 80% spool opening.

Within a certain range of spool opening (±10% in this study), the measured flow versus spool opening curve was approximately linear as shown in Fig. 4(b). Hence, in tests with small spool opening/flow demands, the linear velocity feedback compensation can be viable. Beyond this limit, nonlinearities in the servovalve flow property become significant, and must be considered in the velocity feedback compensation. Specifically, the load pressure influence is significant when the effective force command is large compared with the actuator capacity while the nonlinear flow gain becomes important when the structural velocity is large during a test compared with the maximum piston velocity.

Although the flow property corresponding to an 80% spool opening was identified experimentally and a flow curve was constructed for the whole operating range of the servovalve, it is recommended to use up to 60% spool opening in practice. The reason is that at higher spool openings, the test system becomes less responsive due to a significantly reduced flow gain as shown

Table 2. Flow Curve for the Servovalve (Flow Values in in.^{3}/s, 1 in.^{3}/s=1.64E−5 m^3/s)

x_v	0.1	0.2	0.3	0.4	0.5	0.6	0.7	0.8	0.9	1.0
Q_L+	102.2	187.2	260.4	321.1	369.8	411.2	441.0	468.3	495.7	523.0
Q_L−	−101.0	−188.2	−260.9	−324.2	−377.1	−419.9	−452.3	−480.2	−508.2	−536.2

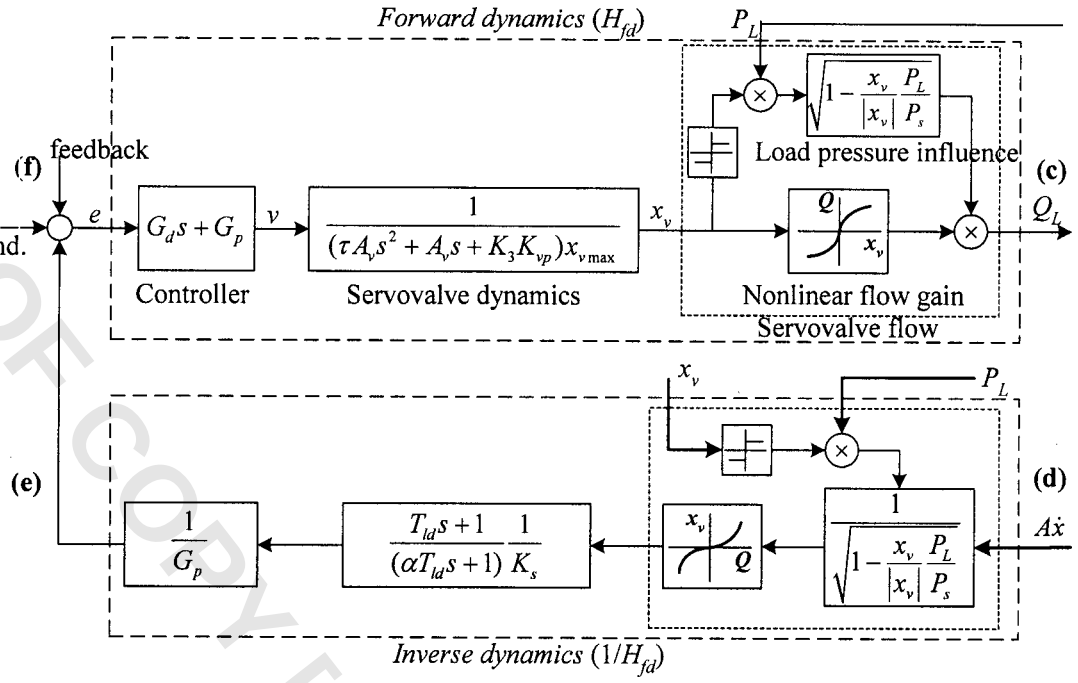

Fig. 5. Nonlinear velocity feedback compensation design

by the flattening of the curve in Fig. 4(b) for spool openings beyond ±60%. Once the nonlinear flow model was identified, a nonlinear velocity feedback compensation scheme was designed accordingly.

Nonlinear Velocity Feedback Compensation

The design of the nonlinear velocity feedback compensation is presented in Fig. 5. The path from point (f) to point (c) shows the forward dynamics formed by three components: the dynamics of the servovalve controller by Eq. (1), the servovalve dynamics by Eq. (4), and the servovalve flow property by Eq. (6) and Table 2. In order to implement the velocity feedback compensation, the inverse of the dynamics of these components was needed.

The inverse flow relationship determines the required spool opening to compensate for the actuator chamber volume variation. The servovalve flow property is nonlinear as shown in Eq. (6) and contains two types of nonlinearities: *nonlinear flow gain* and *load pressure influence*. If the required spool opening and the effective forces are small (i.e., $|x_v| \leq 0.1$ and $|P_L| \leq 0.05 P_s$) such that these nonlinearities are negligible, the inverse flow relationship can be taken as $A\dot{x}/K_v$, where K_v is the initial no-load flow gain (slope of the flow curve at the origin), resulting in a linearized compensation scheme.

Beyond the linear range, the inverse of the nonlinear servovalve flow property was obtained as follows. The chamber volume variation to be compensated ($A\dot{x}$) was first multiplied by $1/\sqrt{1-(x_v/|x_v|)(P_L/P_s)}$ to consider the effect of large forces applied to the structure. This process required two more inputs, the spool opening (x_v) and the load pressure (P_L). The spool opening was obtained directly from the servovalve controller while the load pressure was approximated by the applied force divided by the piston area. A look-up table based on the piecewise linear flow curve was then used to find the required spool opening that would provide the compensation flow to the actuator.

The inverse servovalve dynamics relate the required spool opening to the valve command. The direct inverse of the servovalve dynamics results in a transfer function with a second-order term in the numerator, which may cause stability problems in that it can greatly amplify signals with high frequencies (e.g., 60 Hz electric noise), which in turn may excite the high-frequency servovalve dynamics. Hence a first-order term [$K_s/(T_d s+1)$, where K_s=valve gain] with a time constant (T_d) of 5.0 ms was used to represent the servovalve dynamics for frequencies of interest (0–10 Hz), and a first-order phase-lead network multiplied by $1/K_s$ was used to invert the valve dynamics

$$H(s) = \frac{1}{K_s}\frac{T_{ld}s+1}{\alpha T_{ld}s+1} \quad \text{and} \quad T_{ld} = \frac{T_d}{1-\alpha} \tag{8}$$

where the constant α was taken as 0.1 because it could provide both good phase-lead performance (the performance would be reduced if α was too large) and acceptable noise amplification (noises would be greatly amplified if α was too small). Fig. 6

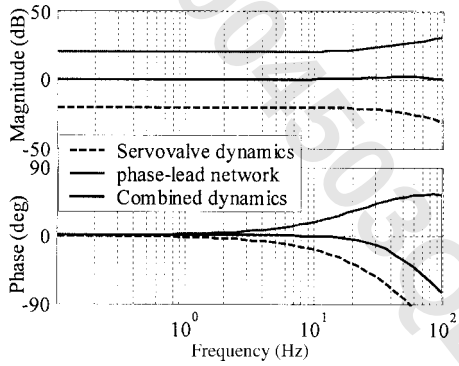

Fig. 6. Frequency responses of the servovalve dynamics and inverse dynamics

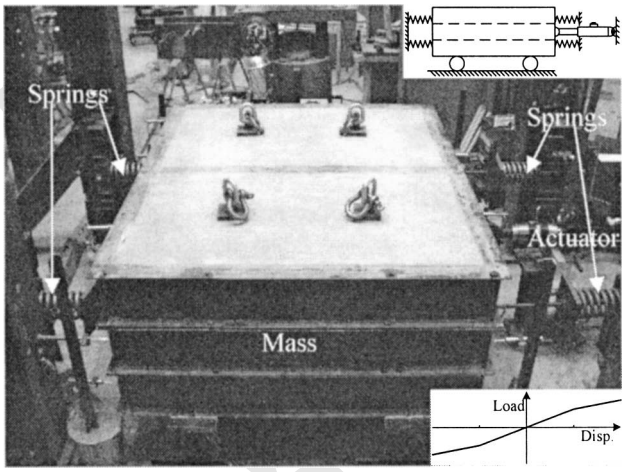

Fig. 7. Single degree-of–freedom test structure with the actuator

presents the frequency responses of the second-order servovalve model and the phase-lead network. The responses (amplitude and phase) of the combined component [i.e., the servovalve model followed by the phase-lead network Eq. (8)] shown in dark solid lines are flat up to 20 Hz, indicating effective inverse dynamics for a wide range of frequencies.

PID controls with a zero I gain introduce some phase lead into the dc error signal if the derivative gain (controller D gain) is not zero. Because D gain was usually set very small (e.g., 0.2 ms) in this study, the controller dynamics were simplified as a pure gain, and the related phase lead was lumped into the dynamics of the servovalve: the lead-time (G_d/G_p) was considered by reducing the servovalve response delay. Hence the inverse dynamics of the servovalve controller was simply $1/G_p$.

Experimental Validation

The nonlinear velocity feedback compensation was verified by testing a SDOF mass-spring-damper structural model shown in Fig. 7. The test structure consisted of a concrete mass atop four caster wheels with two springs on each side of the structure in the direction of motion. The concrete mass weighed 7,040 kg (15.5 kip). The springs were designed to lose contact with the mass at displacements exceeding 25 mm (1 in.), resulting in a reduced stiffness. Thus the structure was a linear elastic structure with a stiffness of 694 kN/m (3.96 kip/in.) when the displacement response was within the 25-mm precompression, while it acted as a nonlinear elastic structure when the displacement response exceeded the precompression [the stiffness reduced to 350 kN/m (2.0 kip/in.)]. A viscous fluid damper was used and an equivalent damping of 3.0% of critical damping obtained from free-vibration tests was used to approximate the system damping property.

Sine Sweep Input

A test was conducted with an 8.9-kN (2.0-kip) sine wave sweep (0–10 Hz) to evaluate the efficiency of the nonlinear velocity feedback compensation design across a range of frequencies. Fig. 8 compares measured forces to command forces in both the time domain and the frequency domain. Only a portion of the response in the time domain (from 4 to 8 s) is presented to facilitate the comparison. In this test, the maximum spool opening was approximately 55%, which was beyond the linear range of the servovalve flow gain (10%). With the nonlinear velocity feedback compensation, no obvious difference between force output and the command was identified in the time domain though the force measurement was noisy. In the frequency domain, the fast Fourier transform (FFT) of the measured force does not show any obvious drop across the whole frequency range, indicating that the actuator was able to follow the force command at all frequencies (0–10 Hz).

The results of a test and a corresponding simulation with the linearized compensation, in which the velocity feedback compensation was based on the initial servovalve flow gain instead of the nonlinear flow curve, are also shown in Fig. 8 for comparison. A sharp drop in the amplitude of the FFT of the force output is evident around 1.6 Hz for the linearly compensated system in the frequency domain, indicating that nonlinear compensation is necessary. The computer simulation used the proposed nonlinear ser-

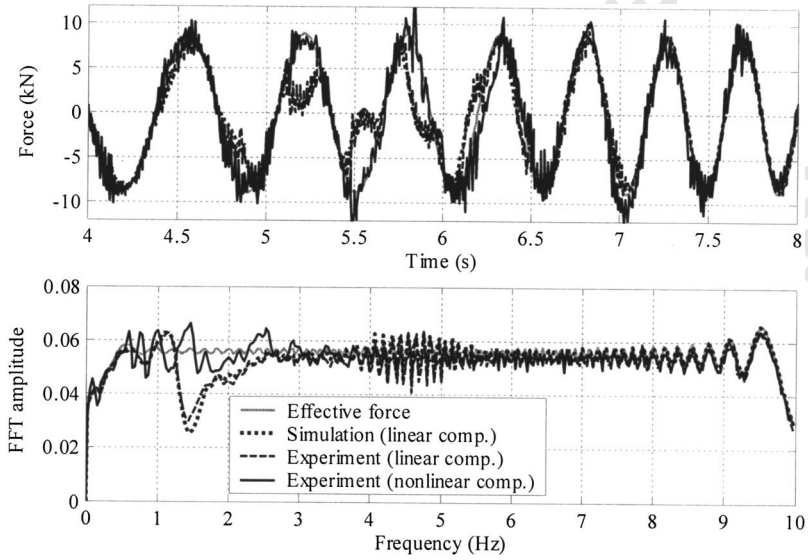

Fig. 8. Compensation of velocity feedback compensation schemes

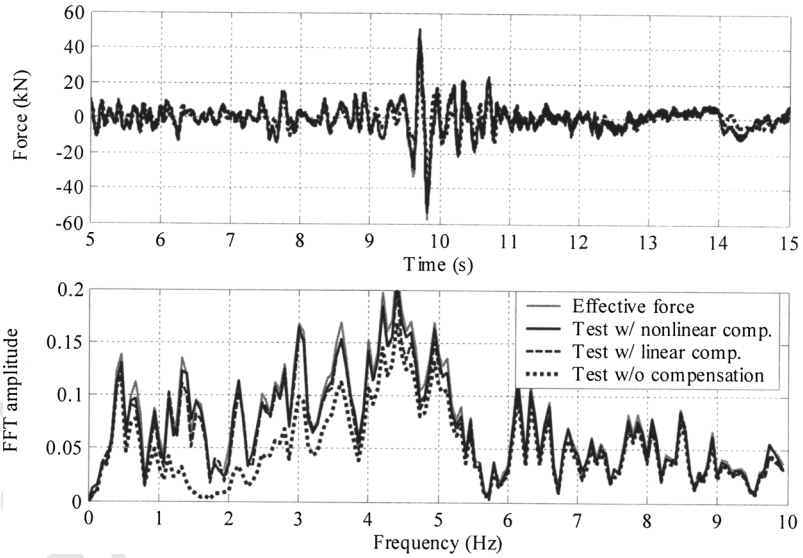

Fig. 9. Test results with various velocity feedback compensation schemes (0.84g Northridge)

vovalve model and identified parameters in the forward dynamics and the linearized velocity feedback compensation. The close match between the test results and the simulation results indicates that the model accurately described the system behavior.

Earthquake Effective Force Inputs

Tests were also conducted with the full-scale 1994 Northridge earthquake ground acceleration (0.84g), and results are shown in Figs. 9 and 10. With the nonlinear velocity feedback compensation, the measured force matched the force command closely in the time domain, and the measured displacement and velocity responses generally followed and were in phase with the desired responses though several response peaks were not fully reached. The differences were partially due to inaccuracies in structural modeling (e.g., using linear viscous damping to represent the complicated fluid damper behavior) and partially due to the incomplete compensation of natural velocity feedback.

For comparison purposes, test results with the linear compensation and without velocity feedback compensation are illustrated in the same plot. The actuator appeared to follow the force commands in the time domain, even in the case without implementation of any velocity feedback compensation. However, if the natural velocity feedback was not compensated, the frequency content near structural resonance was significantly lower than the desired level as shown by the dotted lines in Fig. 9, and the structural responses were significantly smaller than the desired responses in Fig. 10. With the linear velocity feedback compensation, response amplitudes were improved, but still were below those of the test with nonlinear compensation. In addition, the system developed a very different deformation pattern after 11 s. The large discrepancy in the structural responses was attributed to inaccurate forces applied to the structure and the fact that nonlinear structural responses are dependent on the loading history.

A reason for the incomplete compensation even with the non-

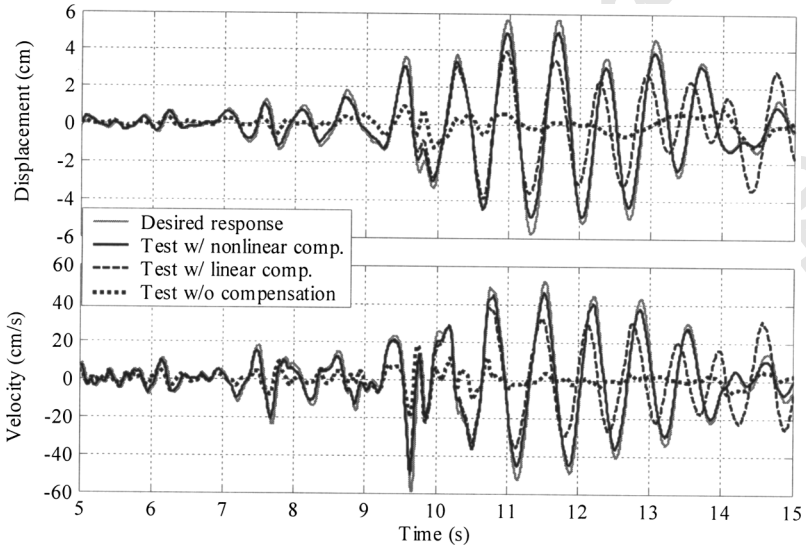

Fig. 10. Structural responses in test with various velocity feedback compensation schemes (0.84g Northridge)

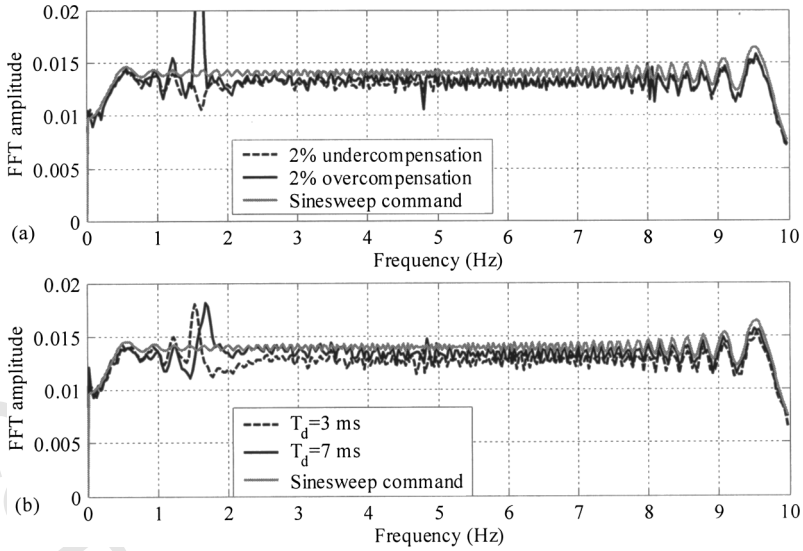

Fig. 11. (a) Effect of various velocity feedback compensation levels, and (b) effect of various delay compensation levels

linear velocity feedback compensation is that the proposed compensation scheme required accurate knowledge (model) of the servovalve while uncertainties exist in the physical system that can affect the performance of the compensation scheme. Therefore it is necessary to investigate the ability of the compensated test system to accommodate variations in system parameters.

Discussion of System Uncertainties

The implementation of the velocity feedback compensation schemes requires the following parameters: controller P gain (G_p), servovalve gain (K_s), servovalve response delay (T_d), and servovalve flow versus spool opening relationship. Two parameters, the response delay and the flow property of the servovalve, are briefly discussed because they have the largest uncertainties.

Servovalve Flow Gain

The servovalve flow property may vary due to uncertainties in the test environment (e.g., hydraulic supply, etc.) as shown in Fig. 4(b) while the compensation is based on a predetermined flow curve. Hence, the natural velocity feedback may be either slightly undercompensated or overcompensated during a test. The effect of the flow property variation is shown in Fig. 11(a), which compares the test results of the system subjected to a 2.2 kN sine wave sweep input with different compensation levels. Slight undercompensation (2%) resulted in some amplitude reduction at the natural frequency while 2% overcompensation caused the overshoot of the force at the natural frequency. It should be noted that the large spike at the natural frequency was in part attributed to the fact that the overcompensation contaminated the valve command signal with small signals at that frequency (from the structural velocity response), and the accumulating process of the FFT calculation built up a spike at that frequency.

An overcompensated system may become unstable, and the unstable vibration at a frequency close to the structural resonant frequency can cause unwanted damage to the test structure. The stability margin of the system, indicating the maximum tolerable overcompensation, is dependent on structural damping. Higher structural damping helps to stabilize the test system and increase the tolerable level of the system identification error (Zhao 2003).

Servovalve Response Delay

Similar to the main-stage valve flow property, the pilot-stage valve can be affected by the variation of the hydraulic supply, which in turn may affect the response delay of the three-stage servovalve. Therefore slight under- or over-compensation of the servovalve response delay is likely to happen when the compensation using the phase-lead network is based on a predetermined time constant.

As mentioned previously, a time delay of 5 ms was optimal for the servovalve in this study. To investigate the effect of the variation of the compensated time delay, tests with 3- and 7-ms compensation were conducted, and results are illustrated in Fig. 11(b). With insufficient delay compensation, a peak before a valley appeared in the FFT near the structure's natural frequency of the measured force while a peak after a valley appeared in the frequency domain when the delay was overcompensated. This information can be useful when searching for the optimal time constant for the phase-lead network.

Compared to the case of the flow gain, the system has a wider stability margin with respect to the response delay compensation. However, undercompensation of the response delay may destabilize a high-frequency vibration mode (around 60 Hz for this study though not shown here). This unstable vibration mode would not damage the test structure because the frequency is far away from the resonant frequency of the test structure while it may cause noisy force output (Zhao 2003).

Conclusions

To make the implementation of EFT successful, velocity feedback compensation is necessary to negate the effect of the natural velocity feedback. The compensation was made by modifying the command signal to the servovalve controller, which required an accurate knowledge of the servovalve and its controller. The servovalve has high-order dynamics and a nonlinear flow property,

which can have a significant impact on the performance of the EFT method, especially in tests with large hydraulic flow demands usually caused by large structural velocities and/or effective forces. A second-order model can represent the servovalve dynamic behavior for a wide range of frequencies. In addition, a piecewise linear flow curve based on experimental results can represent the servovalve flow property well over the major operating range of the servovalve.

Experimental tests with a nonlinear-elastic SDOF mass-spring-damper structure (that can be either linear or nonlinear elastic) demonstrated that with the proposed nonlinear velocity feedback compensation, real-time dynamic tests can be performed using the EFT method on structures that require large flow demands.

Acknowledgments

Funding for this research was partly provided by the National Science Foundation (NSF) under Grant No. CMS-9821076. The Doctoral Dissertation Fellowship support provided by the 3M Corporation through the Graduate School at the University of Minnesota is acknowledged. However, information contained herein does not necessarily represent the views of the sponsors.

Notation

The following symbols are used in this paper:

A = actuator piston area;
A_v = main-stage spool area;
C_d = load flow orifice discharge coefficient;
C_l = total leakage coefficient;
C_{ip} = internal leakage coefficient;
C_{ep} = external leakage coefficient;
e = external dc error signal;
e_i = internal dc error signal;
G_p = proportional gain setting of the PID controller;
G_d = derivative gain setting of the PID controller;
H_{fd} = forward dynamics model;
H_c = servovalve controller model;
H_{vp} = pilot-stage valve model;
H_{sm} = main-stage valve model;
H_s = overall servovalve dynamics model;
K_a = compressibility coefficient of the hydraulic fluid;
K_{vp} = flow gain of the pilot-stage valve;
m, c, k = structural parameters;
P_L = load pressure (pressure difference across actuator piston);
P_s = hydraulic pressure supply;
P_1, P_2 = chamber pressures;
Q_1, Q_2 = flow to the actuator;
Q_L = load flow;
Q_{lv} = valve leakage flow;
r, c, e = geometric coefficients of the leakage flow orifice;
T_d = servovalve response delay;
T_{ld} = response delay compensation coefficient;
V_1, V_2 = volume of actuator chambers;
w = area gradient (perimeter) of the valve spool;
x_v = main-stage valve spool opening;
$x_{v\,\max}$ = maximum spool stroke;
α = constant of the phase-lead network;
ζ = apparent damping of servovalve;
μ = fluid viscosity;
ρ = mass density of the hydraulic fluid;
τ = equivalent time constant of the pilot-stage valve; and
ω_n = apparent natural frequency of servovalve.

References

Dimig, J., Shield, C., French, C., Bailey, F., and Clark, A. (1999). "Effective force testing: A method of seismic simulation for structural testing." *J. Struct. Eng.*, 125(9), 1028–1037.

Dyke, S. J., Spencer, B. F., Quast, P., and Sain, M. K. (1995). "Role of control-structure interaction in protective system design." *J. Eng. Mech.*, 121(2), 322–338.

Franklin, G. F., Powell, J. D., and Emami-Naeini, A. (1994). *Feedback control of dynamic systems*, 3rd Ed., Addison-Wesley, Boston.

Merritt, H. E. (1967). *Hydraulic control systems*, Wiley, New York.

Murcek, J. A. (1996). "Evaluation of the effective force testing method using a SDOF model." Master's thesis, Civil Engineering, University of Minnesota, Twin cities.

Nikiforuk, P. N., Ukrainetz, P. R., and Tsa, S. C. (1969). "Detailed analysis of a two-stage four-way electrohydraulic flow-control valve." *J. Mech. Eng. Sci.*, 11(2), 168–174.

Shield, C., French, C., and Timm, J. (2001). "Development and implementation of the effective force testing method for seismic simulation of large-scale structures." *Philos. Trans. R. Soc. London, Ser. A* (Theme issue on dynamic testing of structures), 359, 1911–1929.

Thayler, W. J. (1965). "Transfer functions for Moog servovalves." *Technical Bulletin 103*, Moog Inc. controls division, East Aurora, N. Y.

Timm, J. (1999). "Natural velocity feedback correction for effective force testing." Master's thesis, Civil Engineering, University of Minnesota, Twin cities.

Zhao, J. (2003). "Development of EFT for nonlinear SDOF systems." PhD thesis, Civil Engineering, University of Minnesota, Twin cities.

Zhao, J., French, C., Shield, C., and Posbergh, T. (2002). "Development of EFT for nonlinear SDOF systems." *Proc., 7th National Conf. on Earthquake Engineering*, Boston.

Zhao, J., French, C., Shield, C., and Posbergh, T. (2003a). "Nonlinear velocity compensation for effective force testing." *Proc., 2003 Structural Congress and Exhibition*, Seattle.

Zhao, J., French, C., Shield, C., and Posbergh, T. (2003b). "Considerations for the development of real-time dynamic testing using servo-hydraulic actuation." *Earthquake Eng. Struct. Dyn.*, 32(11), 1773–1794.

PROOF COPY [EM/2003/023636] 004503QEM